

6.5 A 3dB-NF 160MHz-RF-BW Blocker-Tolerant Receiver with Third-Order Filtering for 5G NR Applications

Montazerolghaem, Mohammad Ali; Pires, Sergio; De Vreede, Leo C.N.; Babaie, Masoud

DOI

[10.1109/ISSCC42613.2021.9365849](https://doi.org/10.1109/ISSCC42613.2021.9365849)

Publication date

2021

Document Version

Accepted author manuscript

Published in

2021 IEEE International Solid-State Circuits Conference, ISSCC 2021 - Digest of Technical Papers

Citation (APA)

Montazerolghaem, M. A., Pires, S., De Vreede, L. C. N., & Babaie, M. (2021). 6.5 A 3dB-NF 160MHz-RF-BW Blocker-Tolerant Receiver with Third-Order Filtering for 5G NR Applications. In *2021 IEEE International Solid-State Circuits Conference, ISSCC 2021 - Digest of Technical Papers* (pp. 98-100). Article 9365849 (Digest of Technical Papers - IEEE International Solid-State Circuits Conference; Vol. 64). Institute of Electrical and Electronics Engineers (IEEE). <https://doi.org/10.1109/ISSCC42613.2021.9365849>

Important note

To cite this publication, please use the final published version (if applicable).
Please check the document version above.

Copyright

Other than for strictly personal use, it is not permitted to download, forward or distribute the text or part of it, without the consent of the author(s) and/or copyright holder(s), unless the work is under an open content license such as Creative Commons.

Takedown policy

Please contact us and provide details if you believe this document breaches copyrights.
We will remove access to the work immediately and investigate your claim.

6.5 A 3dB-NF 160MHz-RF-BW Blocker-Tolerant Receiver with Third-Order Filtering for 5G NR Applications

Mohammad Ali Montazerolghaem¹, Sergio Pires², Leo de Vreede¹, Masoud Babaie¹

¹Delft University of Technology, Delft, The Netherlands, ²Ampleon, Nijmegen, The Netherlands

The introduction of the fifth-generation (5G) New Radio (NR) standard has imposed several challenges in the design of sub-6GHz receivers (RX). Firstly, the maximum channel bandwidth (2BW) increases to 100MHz, while a -15dBm continuous wave (CW) blocker can be located only $\Delta f=85\text{MHz}$ away from the desired band edge. Such a small $\Delta f/\text{BW}$ (~ 2) places a stringent linearity requirement on an RX, and thus demanding the use of higher-order filtering. Secondly, in-band (IB) linearity also becomes critical, since the band of interest may contain many signals resulting from carrier aggregation and digital beamforming operation. Finally, a sub-3dB noise figure (NF) is required to achieve the highest possible link budget, which allows to maximize the spectral efficiency and data rate.

Mixer-first architectures are traditionally considered as appealing candidates for 5G RXs due to their simplicity, low power consumption (P_{DC}), and most importantly, high out-of-band (OB) linearity [1-2]. However, their NF is poor, degrading the link budget. Moreover, as the input impedance (Z_{in}) of the baseband TIAs should satisfy the input matching, the RX IB linearity is eventually limited by the signal swing at TIA's input. Adding an auxiliary noise-canceling path alleviates this issue [3], at the cost of $\sim 2\times$ larger P_{DC} as the number of wideband TIAs is doubled. Furthermore, LO consumes a considerable power to drive large mixer switches as their on-resistance (R_{sw}) noise cannot be canceled. On the contrary, LNTA-based RXs provide a better trade-off between NF, gain, and P_{DC} . However, to achieve the required IB and OB linearity, additional mechanisms are required to effectively filter close-in blockers at the LNTA's input and output ports. In this paper, we propose to add two programmable zeros and an auxiliary current-sinking path in the LNTA feedback to filter nearby and far-out blockers, respectively. To further improve OB linearity and achieve a flat IB response, a second-order TIA with complex-conjugate poles is also introduced.

Several attempts have been made to improve the linearity of LNTA-based RXs (Fig.1). Two bandpass N-path filters are utilized at the LNTA's ports in [4]. However, the OB LNTA gain (G_{LNTA}) and the ultimate input rejection will be limited by R_{sw} , imposing a strong tradeoff between area, LO power, and linearity. A more promising solution is to place a band-stop N-path filter in the LNTA's feedback [5-6]. In this way, a larger transconductance gain of LNTA (G_m) simultaneously results in better NF and OB rejection, as the far-out OB Z_{in} is $\sim 1/G_m$. More interestingly, if $R_{sw}=1/G_m$, OB G_{LNTA} will not flatten. Nevertheless, this condition again bonds the OB Z_{in} to R_{sw} , thus still facing the same tradeoff as in the first structure. Moreover, both Z_{in} and G_{LNTA} have $\sim 20\text{dB/dec}$ roll-off, offering limited rejection for close-in blockers, which is demanded by 5G NR applications. To increase the filter selectivity through steeper transition-band roll-off, we propose to add two zeros to the LNTA's feedback impedance (see Fig.1-bottom). The feedback impedance comprises a parallel resonator (L_p, C_p) in series with a series tank (L_s, C_s), both resonating at the desired frequency (ω). The frequency of the zeros can be manipulated to be close to the desired band using: $\omega_{z1}=1/\sqrt{L_p C_s}$, and $\omega_{z2}=1/\sqrt{L_s C_p}$. This structure offers much better rejection at both LNTA input and output for $|\Delta f/\text{BW}>2$ (see Fig.1). Beyond this span, its performance degrades, which its remedy is discussed later.

The next step is to replace the resonators with tunable filters. The parallel tank can be easily realized by a band-stop N-path filter. Consequently, to have a synthesizable network, we replace the series LC tank with its counterpart, i.e., a gyrator in series with a parallel LC tank, as shown in Fig.2. Each parallel resonator is then replaced with an 8-path switched-capacitor N-path filter clocked at ω_b . In the new network, the zeros frequencies occur at $\omega_0\sqrt{1\pm\sqrt{(g_{ma}g_{mb})/(C_T\omega_0^2)}}$, where C_T is the equivalent capacitance of the N-path filter, while g_{ma} and g_{mb} are the feedforward and feedback transconductance of the gyrator, respectively. Interestingly, the zeros frequencies can be tuned by the product of g_{ma} and g_{mb} and their corresponding noise does not degrade NF due to the attenuation of the band-stop filters. As mentioned earlier, this structure is only beneficial for close-in blockers, since both Z_{in} and G_{LNTA} rapidly go up beyond $|\Delta f/\text{BW}>2$. To resolve this issue, we added an extra band-stop N-path filter from the antenna to the gyrator's second port. Its BW is intentionally chosen larger than that of the main filters such that this extra path acts as an open circuit for the desired band and the close-in blockers, maintaining their frequency response. However, for $|\Delta f/\text{BW}>2$, the auxiliary path shorts the gyrator; thus the frequency response of the system becomes similar to the LNTA with a simple band-stop filter in the feedback, removing the effect of zeros in Z_{in} and G_{LNTA} at

far-out frequencies. Consequently, the close-in blockers are attenuated heavily by the zeros, while the current of far-out blockers is sunk to ground through the extra path.

Fig.3 shows the circuit implementation of the proposed current-mode RX. The RF current of the bandpass LNTA (BLNTA) is down-converted by using passive mixers that are driven with 8-phase non-overlapping clocks to reject the 3rd and 5th LO harmonics, thereby improving NF. The TIAs use a new second-order inverter-based amplifier topology with complex-conjugate poles to provide flat IB response and enhance OB linearity. As depicted in Fig.3, in this work, the feedback capacitance of the conventional first-order TIAs is removed and another capacitor (C_L) is placed at the TIA output. This gives us another degree of freedom to realize a trans-impedance filter with complex-conjugate poles, and $\text{BW} \approx \sqrt{(g_{m,TIA}/(R_T C_L))}$. Compared to the conventional design, this filter requires more capacitance for certain BW. However, as the channel BW is relatively large in 5G radios, the chip area increases negligibly. Moreover, a sufficiently high $g_{m,TIA}$ guarantees enough phase margin for the filter, avoiding instability but at the cost of potentially higher power consumption.

Harmonic rejection is performed by combining the TIAs outputs with weighted factors. To decouple input matching from the BLNTA's noise and linearity, the 50Ω matching is realized by upconverting baseband signals at TIA outputs and feeding them back to BLNTA input through R_m resistors. Consequently, BLNTA IB voltage gain can be relatively low to suppress the voltage swing at its output, thus improving RX linearity. Moreover, R_m contribution to the NF is negligible due to the large voltage gain of the entire RX.

The RX fabricated in 40nm CMOS occupies a core area of 0.6mm^2 (Fig.7). The measured S_{11} and LO leakage are respectively $<-18\text{dB}$ and $<-69\text{dBm}$ over the 0.4-to-3.2GHz RF range (Fig. 4). The NF measures down to 2.7dB at 0.5GHz, and up to 3.6dB at 3.0GHz. With a 0dBm CW blocker injected at $|\Delta f/\text{BW}=6.25$, the NF increases to 8.3dB. The worst-case in-band measured gain and -3dB baseband BW are 30dB and 80MHz, respectively. The transfer function of RX gain has $\sim 60\text{dB/decade}$ OB roll-off, which extends up to $|\Delta f|=0.8\text{GHz}$. IIP3/IIP2 is $-19\text{dBm}/13\text{dBm}$ in-band, and rapidly reaches 8dBm/40dBm for $|\Delta f/\text{BW}=2$, thanks to the 2nd-order TIA and LNTA feedback impedance (Fig.5). When the auxiliary path is ON, the input matching is restricted to the desired band, and far-out OB-IIP3/B1dB reach $+13\text{dBm}/-5\text{dBm}$. With a -60dBm 143MSym/s (0.85Gb/s) 64-QAM OFDM input signal, the RX EVM only degrades from -26.4dB to -25.5dB when a -8dBm blocker is applied at $|\Delta f/\text{BW}=5$.

Benchmarking with prior LNTA-based RXs [5-7] (Fig.7), this work offers the highest filtering order and flat BW, while maintaining a low NF. Comparing to the recent mixer-first RXs with a comparable BW and filtering order [2], OB IIP3 and P_{DC} of our RX are worse but it shows a better NF, blocker NF, and RF input range without utilizing a large supply voltage or any off-chip components. This work is also the only one that demonstrates the overall RX performance by measuring the EVM with and without a blocker.

Acknowledgment

This work was supported by the Netherlands Organization for Scientific Research (NWO) under project 16336. The authors would like to thank Atef Akhrouk and Zu Yao Chang from Delft University of Technology for tape-out/measurement support, and Sajad Golabi and Zhong Gao for their useful suggestions.

References:

- [1] Y. Lien *et al.*, "Enhanced-Selectivity High-Linearity Low-Noise Mixer-First Receiver With Complex Pole Pair Due to Capacitive Positive Feedback," *IEEE JSSC*, vol. 53, no. 5, pp. 1348-1360, May 2018.
- [2] G. Pini *et al.*, "Analysis and Design of a 260-MHz RF Bandwidth $+22\text{-dBm}$ OOB-IIP3 Mixer-First Receiver With Third-Order Current-Mode Filtering TIA," *IEEE JSSC*, vol. 55, no. 7, pp. 1819-1829, July 2020.
- [3] A. N. Bhat *et al.*, "A Baseband-Matching-Resistor Noise-Canceling Receiver Architecture to Increase In-Band Linearity Achieving 175MHz TIA Bandwidth with a 3-Stage Inverter-Only OpAmp," *IEEE RFIC*, 2019, pp. 155-158.
- [4] A. Mirzaei *et al.*, "A 65 nm CMOS Quad-Band SAW-Less Receiver SoC for GSM/GPRS/EDGE," *IEEE JSSC*, vol. 46, no. 4, pp. 950-964, April 2011.
- [5] H. Wang *et al.*, "A Wideband Blocker-Tolerant Receiver with High-Q RF-Input Selectivity and $<-80\text{dBm}$ LO Leakage," *IEEE ISSCC*, 2019, pp. 450-452.
- [6] J. W. Park *et al.*, "Channel Selection at RF Using Miller Bandpass Filters," *IEEE JSSC*, vol. 49, no. 12, pp. 3063-3078, Dec. 2014.
- [7] J. Musayev *et al.*, "A Quantized Analog RF Front End," *IEEE JSSC*, vol. 54, no. 7, pp. 1929-1940, July 2019.

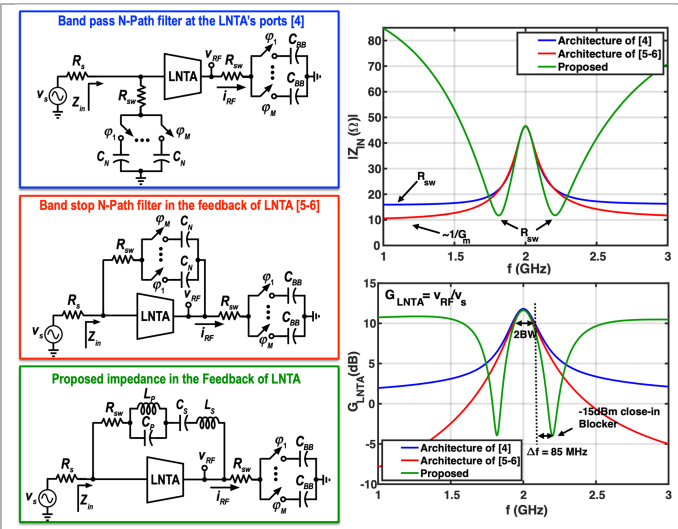


Figure 6.5.1: Prior art (top/middle-left) and the proposed architectures (bottom-left) for improving the OB linearity of LNTA-based receivers; Comparison between the simulation results of the RX Z_{in} and G_{LNTA} for different structures.

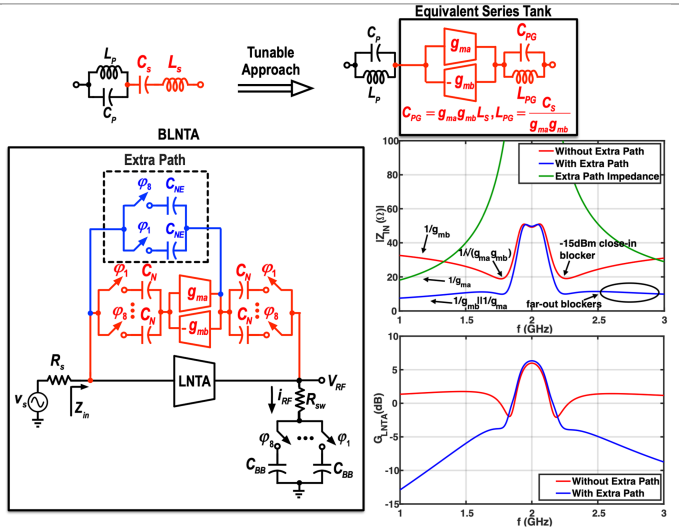


Figure 6.5.2: Evolution of the proposed BLNTA to achieve an adjustable center frequency and bandwidth; Comparison between the simulation results of the RX Z_{in} and G_{LNTA} with and without the extra path.

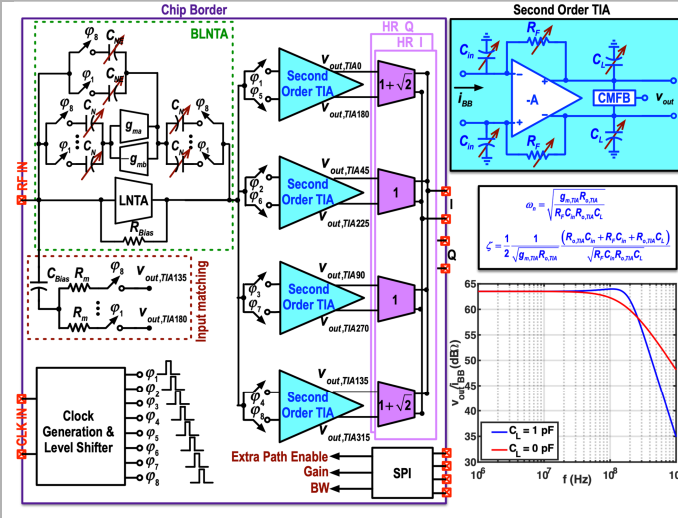


Figure 6.5.3: The block diagram of the proposed receiver (Left); Schematic of the proposed second-order TIA with complex-conjugate poles and its simulated transfer function (Right).

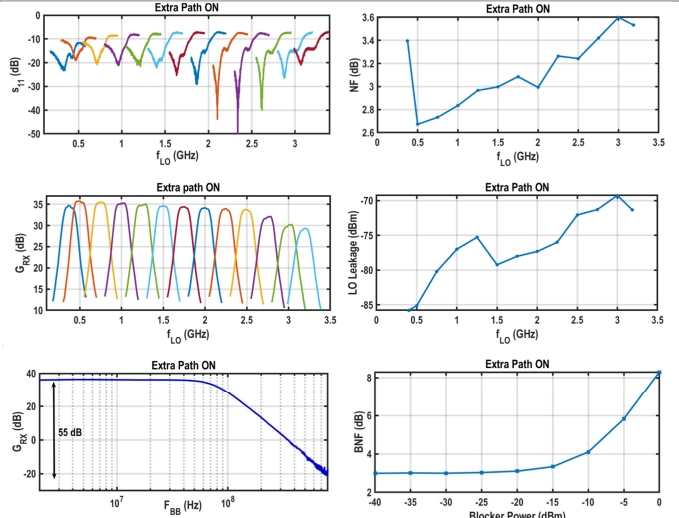


Figure 6.5.4: Measured S_{11} , NF, G_{RX} , and LO Leakage vs. LO frequency, BNF vs. blocker power, and G_{RX} versus the baseband frequency, (top-left to bottom right figure).

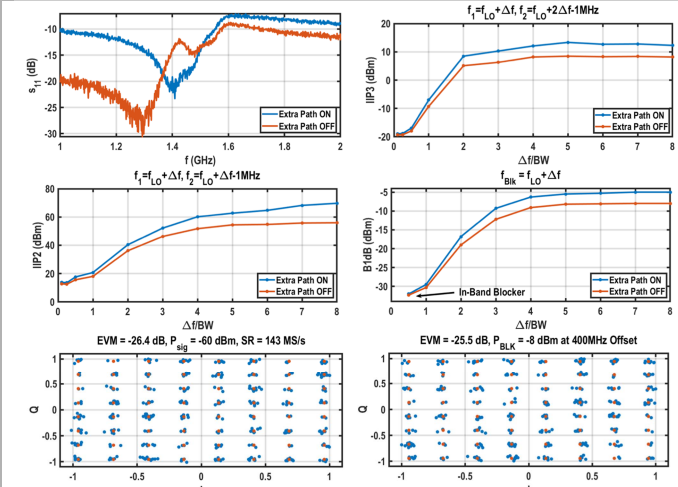


Figure 6.5.5: Effect of the extra path on the measured S_{11} , OB-IIP3, OB-IIP2, and B1dB (top four figures), and EVM measurements with and without blocker (bottom figures).

	This Work	ISSCC 2019 [5]	JSSC 2014 [6]	JSSC 2019 [7]	JSSC2020 [2]	RFIC2019 [3]
Architecture	LNTA Based	LNTA Based	LNTA Based	LNTA Based	Mixer First	Mixer First
Technique	Second Order TIA with zero	Gm boosting N-path filter	Gain Boosted N-path filter	Quantized RX	Third Order Current Mode Filtering	Noise Canceling in BB
Technology	40 nm CMOS	45 nm FDSOI	65 nm CMOS	65 nm CMOS	28 nm CMOS	22 nm FDSOI
f_{RF} (GHz)	0.4 – 3.2	0.2 - 2	0.05-2.5	0.7-1.4	0.5 - 2	1 - 6
Gain (dB)	36	40	38	36.8*20.8*	32.4	22
NF (dB)	2.7-3.6	2.1-2.5	2.9	1.9*14.6*	5.5	2.5 - 5
S_{11} (dB)	< -18	< -10	< -10	-	< -13	< -10
LO Leakage (dBm)	< -69	< -80	< -67	-	-	-
BB BW (MHz)	80	10	1	1	130	175
Flat BW	Yes	No	Yes	No	Yes	No
Filtering Order	-60 dB/dec	-40 dB/dec	-40 dB/dec	-20 dB/dec	-60 dB/dec	-20 dB/dec
OB IIP3 (dBm)	13	14	10	20.5*	21	18
	$\Delta f/BW = 5$	$\Delta f/BW = 10$	$\Delta f/BW = 100$		$\Delta f/BW = 3$	$\Delta f/BW = 5.7$
OB IIP2 (dBm)	70	60	58	75*	70	-
0 dBm BNF (dB) (at offset)	8.4	6.7	5.1	6.6*7.9*	10	-
	($\Delta f/BW = 6.25$)	($\Delta f/BW = 8$)	($\Delta f/BW = 20$)	($\Delta f/BW = 100$)	($\Delta f/BW = 8$)	
EVM w/o/w/ blocker	-26.4/-25.5*	-	-	-	-	-
Supply (V)	1.3/1.2	1.2	1.2	0.8/1/1.2	1.8/1.2	0.83
Active Area (mm ²)	0.6	1.05	0.82	0.25	0.16	0.48
Input matching balun	No	No	No	No	Yes	Yes
Power (mW)	58.5 + 17.6 mW/GHz	68-95	20	14+37.2mW/GHz	21.6 + 7.8 mW/GHz	172

Figure 6.5.6: Comparison with the state-of-the-art LNTA-based receivers and mixer first receivers with comparable bandwidth.

§: Low noise mode. * Linear mode. †: at 2GHz. ‡: -8dBm CW blocker at 400 MHz offset ($\Delta f/BW = 5$).

Power Consumption Chart

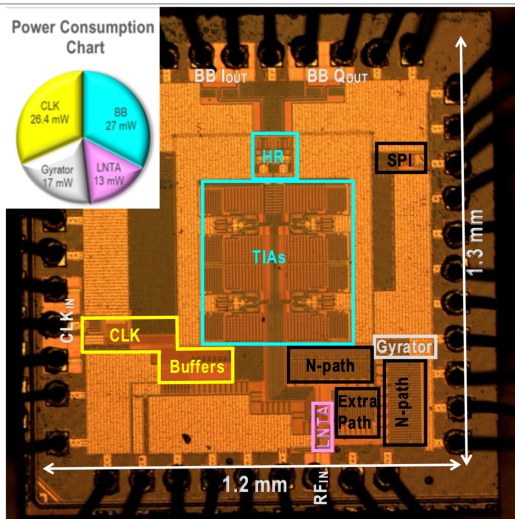
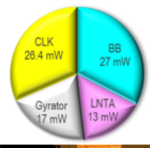


Figure 6.5.7: Die micrograph and power consumption summary at 1.5 GHz.